

calculated boundary voltages are processed in the same way as that for the measured data.

Using the modified algorithm, we have reconstructed images from the measured data corresponding to the objects in Figs. 2a and b, respectively. The images in Figs. 2c and d are the reconstructions of the objects in Figs. 2a and b, where the grey levels give the relative conductivity within each image. An assumed uniform conductivity distribution is used for starting the iteration in the two experiments, which is the practical initial distribution when little *a priori* knowledge of the object is known.

**Conclusions:** By locally normalising the measured data and modifying the original reconstruction algorithm, the compatibility between the measured data and the iterative algorithm has been improved and meaningful reconstructions can be generated.

The modified algorithm still uses a discrete model to replace the continuous object, and hence a slight modelling error is inevitable. Theoretically, the modelling error can be reduced to zero by refining the discretisation of the object but this will greatly increase the numerical error of the reconstruction because of the increased number of unknowns in the non-linear inverse problem. A compromise is therefore necessary to obtain an effective reconstruction.

Z. Q. CHEN  
F. J. PAOLONI

17th November 1988

Department of Electrical & Computer Engineering  
University of Wollongong  
PO Box 1144, NSW 2500, Australia

#### References

- 1 BARBER, D. C., BROWN, B. H., and FREESTON, I. L.: 'Imaging spatial distributions of resistivity using applied potential tomography', *Electron. Lett.*, 1983, **19**, pp. 933-935
- 2 BARBER, D. C., and BROWN, B. H.: 'Applied potential tomography', *J. Phys. E: Sci. Instrum.*, 1984, **17**, pp. 723-731
- 3 MURAI, T., and KAGAWA, Y.: 'Electrical impedance computed tomography based on a finite element model', *IEEE Trans.*, 1985, **BME-32**, pp. 177-184
- 4 YORKEY, T. J., WEBSTER, J. G., and TOMPKINS, W. J.: 'Comparing reconstruction algorithms for electrical impedance tomography', *ibid.*, 1987, **BME-34**, pp. 843-852

## NEW CONSTRUCTION OF COSTAS SEQUENCES

*Indexing terms:* Codes, Sequences, Frequency-hopping, Radar, Signal processing, Information theory

A new construction of Costas sequences, based on the logarithm of the linear congruence function over  $GF(p)$ , when  $p$  is prime, is presented. It is shown that for every prime  $p$ , the set of  $p-1$  Costas sequences of length  $p-1$  can be generated.

**Introduction:** A Costas signal is a burst of  $N$  contiguous CW pulses of duration  $T$ , each at a different frequency selected from the finite set of  $N$  equally spaced frequencies. The order in which the frequencies are emitted greatly influences the ambiguity function of the burst. A frequency spacing equal to the reciprocal of the pulse duration, in combination with a uniform pulse envelope, also has significance in terms of the ambiguity function behaviour. The sequence of frequencies in a Costas signal produces an optimum ambiguity function.<sup>1</sup> Therefore Costas sequences are the best sequences for applications in frequency-hopping radar and sonar systems.

The problem of constructing Costas sequences can be stated in the following manner:<sup>1</sup> order the complete set of integers from 1 to  $N$  such that the difference triangle formed from the ordered sequence shall have no repeated terms in any row.

Thus defined, a frequency-hopping sequence has no more than one coincidence with its time- and frequency-shifted versions.

If we represent a sequence of integers as

$$\{f_i\} = f_1, f_2, f_3, \dots, f_N \quad (1)$$

then the  $t$ th row of the difference triangle will contain elements  $D_{t,i}$ , defined as

$$D_{t,i} = f_{i+t} - f_i \\ t = 1, 2, 3, \dots, N-1 \quad i = 1, 2, 3, \dots, N-t \quad (2)$$

The frequency-hopping sequence  $\{f_i\}$  is a Costas sequence if the following condition is satisfied:<sup>1</sup>

$$D_{t,r} \neq D_{t,s} \quad \text{for } r \neq s \quad (3)$$

Obviously, the elements of the difference triangle will not change if the sequence elements belong to the set of integers ranging from 0 to  $N-1$ , as in the case of sequences which are produced by the new construction.

A comprehensive survey of the algebraic constructions of Costas sequences (arrays) was given in Reference 2. Recently, another construction of Costas sequences has appeared in the Russian literature.<sup>3</sup> In a sequel, we shall present the systematic algebraic construction of Costas sequences that seems to be still unpublished in the open literature.

**Theorem:** For every prime  $p$ , the set of  $p-1$  Costas sequences of length  $p-1$ , can be generated as follows:

$$\mathcal{S} : \{f_{m,i}\} \quad m = 1, 2, \dots, p-1 \\ f_{m,i} = \log_x(mi) \\ i = 1, 2, \dots, p-1 \quad mi \in GF(p) \quad (4)$$

where  $\{f_{m,i}\}$  is the  $m$ th Costas sequence from the set  $\mathcal{S}$ ,  $f_{m,i}$  is an element of the Costas sequence, and  $\alpha$  is a primitive element of the Galois field  $GF(p)$ . The argument of the logarithm function is computed modulo  $p$ , i.e. according to the rules of  $GF(p)$  when  $p$  is prime.

**Proof:** To prove that the sequence  $\{f_{m,i}\}$  is a Costas sequence, we shall define the 'cyclic' difference triangle, with elements  $D_{t,i}^*$  given as

$$D_{t,i}^* = \{f_{i+t} - f_i\} \bmod p-1 \\ t = 1, 2, 3, \dots, N-1 \quad i = 1, 2, 3, \dots, N-t \quad (5)$$

It is easy to see that if the relation

$$D_{t,r}^* \neq D_{t,s}^* \quad \text{for } r \neq s \quad (6)$$

is valid, then condition expr. 3 is automatically satisfied.

Substituting expr. 4 into eqn. 5, we obtain

$$D_{t,i}^* = \{\log_x [m(i+t)] - \log_x(mi)\} \bmod p-1 \quad (7)$$

$$D_{t,i}^* = \log_x \left[ \frac{i+t}{i} \right] \\ = \log_x [1 + ti^{-1}] \quad (1 + ti^{-1}) \in GF(p) \quad (8)$$

For every  $i \in GF(p)$  there is a unique inverse element  $i^{-1} \in GF(p)$ , so the difference  $D^*$  has different values for every  $i$ , thus satisfying condition expr. 6.

Consequently, the corresponding difference  $D_{t,i}$  will satisfy the condition expr. 3, which means that the sequence  $\{f_{m,i}\}$  is really a Costas sequence.

The new construction is demonstrated in the following example.

**Example:** For  $p = 7$ , one of the primitive elements is  $\alpha = 3$ , so for  $m = 1$  we have

$$\{f_{1,i}\} : 0 \quad 2 \quad 1 \quad 4 \quad 5 \quad 3 \quad (9)$$

and the corresponding difference triangle is

$t$	$D_{t,i}$				
1	2	-1	3	1	-2
2	1	2	4	-1	
3	4	3	2		
4	5	1			
5	3				

(10)

The other Costas sequences from the set are given as follows:

$\{f_{2,i}\}$	: 2	4	3	0	1	5
$\{f_{3,i}\}$	: 1	3	2	5	0	4
$\{f_{4,i}\}$	: 4	0	5	2	3	1
$\{f_{5,i}\}$	: 5	1	0	3	4	2
$\{f_{6,i}\}$	: 3	5	4	1	2	0

(11)

We note that the sequence  $\{f_{4,i}\}$  is the reversed version of sequence  $\{f_{3,i}\}$ , while  $\{f_{5,i}\}$  is the reversed version of  $\{f_{2,i}\}$  and  $\{f_{6,i}\}$  is the reversed version of  $\{f_{1,i}\}$ . This property can be generalised for any prime  $p$ , as

$$\{f_{k,i}\} = \{f_{p-k,p-i}\}$$

$$k = 1, 2, 3, \dots, (p-1)/2 \quad i = 1, 2, 3, \dots, p-1 \quad (12)$$

**Conclusion:** The new construction, which produces the set of  $p-1$  Costas sequences of length  $p-1$ , where  $p$  is prime, is presented. In this set of Costas sequences, there are  $(p-1)/2$  sequences that are nonequivalent under the trivial operation of reversion.

B. M. POPOVIĆ  
*Institute of Applied Physics*  
*B. Lenjina 165b, 11071 Novi Beograd, Yugoslavia*  
 16th November 1988

#### References

- COSTAS, J. P.: 'A study of a class of detection waveforms having nearly ideal range-Doppler ambiguity properties', *Proc. IEEE*, 1984, **72**, pp. 996-1009
- GOLOMB, S. W., and TAYLOR, H.: 'Construction and properties of Costas arrays', *ibid.*, 1984, **72**, pp. 1143-1163
- KOPILOVICH, L. E.: 'On signals with minimal ambiguity function for simultaneous determination of the range and velocity of objects', *Radiotekh. & Elektron.*, 1987, **32**, pp. 1545-1547 (in Russian)

## GaInAsP/InP HETEROJUNCTION BIPOLAR TRANSISTORS WITH A DOUBLE LAYER BASE

*Indexing terms:* Semiconductor devices and materials, Transistors, Bipolar devices

GaInAsP/InP heterojunction bipolar transistors with a double layer base were demonstrated with a direct current gain of 1100 at a collector current density of 110 A/cm<sup>2</sup>. In these particular devices the minority carriers in the base can be transported not only by diffusion but also by drifting.

**Introduction:** Most of the work on GaInAsP/InP heterojunction bipolar transistors (HBTs) has concentrated on a base structure with a single layer.<sup>1-7</sup> In this structure, minority carriers in the base are mainly transported by diffusion. On the other hand, if the composition and/or the doping level is graded in the base region, minority carriers can be transported not only by diffusion but also by drifting. In these graded gap structures, a high current gain and high-speed response can therefore be expected owing to the reduced transit time of minority carriers.<sup>8</sup> It is, however, very difficult to fabricate a compositionally graded base for the GaInAsP/InP system.

Another approach is the use of a base which comprises several layers with different bandgaps. This allows minority carriers to gain substantial kinetic energy every time they come across an interface between layers. The use of a multi-layer base would therefore have the same effect on the performance of the device as the graded bandgap base. Ohnaka *et al.*<sup>9</sup> have recently fabricated HBTs with a base consisting of two layers, the bandgaps of which were 0.95 and 1.13 eV, respectively; they obtained a current gain of 1200 at a current density of 660 A/cm<sup>2</sup>.

To minimise hole injection into the emitter, keeping the transit time of electrons in the base region short, it is desirable to employ a double layer base with smaller bandgaps.

In this letter we report GaInAsP/InP HBTs with a base consisting of two layers, the bandgaps of which are 0.80 and 0.95 eV, respectively. Current gains of 1100 have been attained at a current density of as low as 110 A/cm<sup>2</sup>.

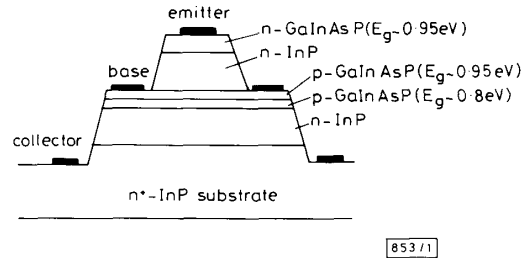


Fig. 1 Schematic cross-section of HBT

**Fabrication and results:** A schematic cross-section of the fabricated transistor structure is shown in Fig. 1. It comprises five layers which were grown on a (100) oriented n<sup>+</sup>-InP substrate by liquid phase epitaxy. The collector consists of an n-InP layer, the thickness of which was 1.2 μm. The free electron concentration of this layer was about 5 × 10<sup>17</sup> cm<sup>-3</sup>. The base is formed by the joint layers p-GaInAsP/p-GaInAsP, the bandgaps of which were 0.8 and 0.95 eV, respectively. The hole concentrations and thicknesses of these layers were p = 9 × 10<sup>17</sup> cm<sup>-3</sup>, d = 0.3 μm and p = 5 × 10<sup>17</sup> cm<sup>-3</sup>, d = 0.2 μm, respectively. An n-InP layer (1.0 μm thick, n = 1 × 10<sup>18</sup> cm<sup>-3</sup>), followed by a quaternary contact layer (0.6 μm thick, n = 1 × 10<sup>19</sup> cm<sup>-3</sup>) was employed for the emitter. Te and Zn were used as n- and p-type dopants, respectively.

After epitaxial growth, to apply ohmic contacts, the wafer was fabricated into a mesa structure as shown in Fig. 1 by conventional photolithography and a selective etching technique. AuGe/Ni/Au and Cr/Au were used for n- and p-layers, respectively. The contacts were not alloyed, because the base-collector junction was found to be degraded by heating at high temperature. The sizes of the emitter-base and collector-base mesas were 180 and 280 μm in diameter, respectively.

Fig. 2 shows the common-emitter current/voltage ( $I_C/V_{CE}$ ) characteristics of the double-layer base HBT. Excellent saturation characteristics can be seen for a collector current up to 30 mA. The turn-on voltage was found to be less than 0.1 V.

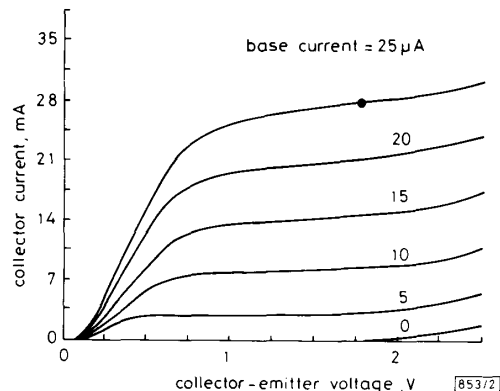


Fig. 2 Common-emitter current/voltage characteristics